Bifurcation to chaos and dimensionality of attractors in an extended Rayleigh-Benard convection system

Bifurcation to chaos and dimensionality of attractors in an extended Rayleigh-Benard convection system

Shinichi Sato
Faculty of Liberal Arts, Shizuoka University, 836 Ohya, Shizuoka 422, Japan

Masaki Sano* and Yasuji Sawada
Research Institute of Electrical Communication, Tohoku University, Sendai 980, Japan
(Received 18 May 1987; revised manuscript received 9 October 1987)

The spatial and temporal bifurcations to chaos and dimensionality of strange attractors in Rayleigh-Benard convection are studied in an extended rectangular container with aspect ratios 15.0 and 1.0. With increasing Rayleigh number, oscillatory states, quasiperiodic states, and chaotic states are observed where the amplitudes of various modes strongly depend on the spatial position. The chaotic states just above the onset are characterized by low-dimensional attractors and the correlation dimension of the attractor is investigated as a function of Rayleigh number.

I. INTRODUCTION

It is generally accepted that the mathematical description of turbulent viscous-fluid flow in a small aspect-ratio container can essentially be reduced to motion of a finite-dimensional dynamical system. Thermal convection in a layer heated from below, the Rayleigh-Benard convection, provides one of the simplest examples of the transition to turbulence in fluid systems. Many experiments have been done on the routes to chaos, including period doubling, intermittency, and quasiperiodicity.[1-8] Furthermore, measurements of the dimension of attractors in chaotic regimes have confirmed the low dimensionality at the onset of chaos in small aspect-ratio systems.[9,10] In large aspect-ratio systems, however, it is not clear whether all phase curves are attracted to a low-dimensional attractor, since the spatial degrees of freedom would be the essential factor. The questions attracting our interest now are how high the dimensions of attractors are, if they exist, and what interplay exists between spatial and temporal structures. We have tried some experimental approaches to answering these questions by measuring the time series of the deviation from the mean gradient of temperature over the whole fluid layer.

Gollub *et al.* have measured the velocity field of the whole layer by using laser Doppler velocimetry both in a small aspect-ratio container[1] and in a large aspect-ratio system.[11] The former experiment was intended to clarify the spatial distribution of the mean flows for the first Hopf bifurcation and the subsequent period-doubling bifurcations. The latter was used to measure the spatial structure of the convection rolls in a steady state. Walden *et al.* observed the development of roll patterns with increasing Rayleigh number for a large aspect-ratio system and saw coexistence of more than three incommensurate frequencies.[12] Held and Jeffries examined the chaotic behavior of an electron-hole plasma in Ge in parallel dc electric and magnetic fields.[13] They asked if the spatially uncorrelated states still corresponded to motion in a phase space along a strange attractor. The correlation integral calculated either from a local signal or from the total current did not show a region of uniform slope for the embedding dimensions they used, and their main question has been left unanswered. In this paper we report measurements of the dimension of attractor which is reconstructed from a local signal of an extended Benard convection system when it shows spatially inhomogeneous fluid motions.

II. EXPERIMENTAL METHODS AND RESULTS

The fluid is confined in a narrow rectangular cell 150-mm wide (x direction), 10-mm deep (y direction), and 10-mm high (z direction), with aspect ratios of $\Gamma_x = 15.0$ and $\Gamma_y = 1.0$. Let the left edge of the bottom plane be the origin of the xy coordinates. The behavior of the fluid in the convection cell with $\Gamma_y = 1.0$ is considerably different from that in the usual large aspect-ratio systems characterized by $\Gamma_x, \Gamma_y \gg 1$, since various instabilities, like cross-roll, zig-zag, and skewed-varicose instabilities are suppressed. This makes the situation simpler. Our extended Rayleigh-Benard convection system is a natural extension of a small aspect-ratio system and elucidates the role of spatial degrees of freedom by simplifying the spatial structure to quasi-one-dimensional geometry. The temperature of the horizontal boundaries on the top and bottom are regulated to within 5 mK. The working fluid is water with Prandtl number $P = 5.5$ at 30 °C. The bifurcation parameter is Rayleigh number R, and we denote the critical Rayleigh number by $R_c = 1708$. Convection rolls with axes perpendicular to the xz plane are generated when R is just above the critical value R_c. The temperature gradient averaged over the y direction is measured by the laser-beam deflection method. The laser beam is moved along the x direction at $z = 3$ mm. The position of each semilocal measurement is represented by the dimensionless parameter L which is a ratio of x to the depth of the fluid container.

In order to characterize the periodic state of the sys-

tem, we chose major peaks in the power spectrum which is normalized by the total power of the time series. The dependence of the peaks on the distance L is shown for different R in Figs. 1(a) and 1(b). We have noticed that there are two types of spatial distribution of spectral power. In the first type (type A), the power is high near one side wall and diminishes toward the other side wall, while the power of the second type (type B) is high near the center of the layer and low near both side walls. When one increases R, one oscillating mode of type A generally appears, as shown in Fig. 1(a). The temperature field of the convection rolls is oscillatory in the left half of the layer, but stationary in right half. At larger R the spatial bifurcation (transition to different spatial structure) is accompanied by a temporal bifurcation. This involves another mode of type A which rises from the other side of the container. In the overlapping region, type-B modes rise simultaneously with relatively small amplitudes and with frequencies corresponding to linear combinations of two type-A modes f_1 (74.4 mHz) and f_1' (68.0 mHz) [Fig. 1(b)]. Further increasing R produces stronger type-B modes. At some particular value of R, nonperiodic oscillations appear and their spectral peaks are broadened. At the same time the power spectra also present the broadband noise.

To investigate nonperiodic fluid motion, the correlation dimension of the attractor is calculated for the locally measured time series by the method proposed by

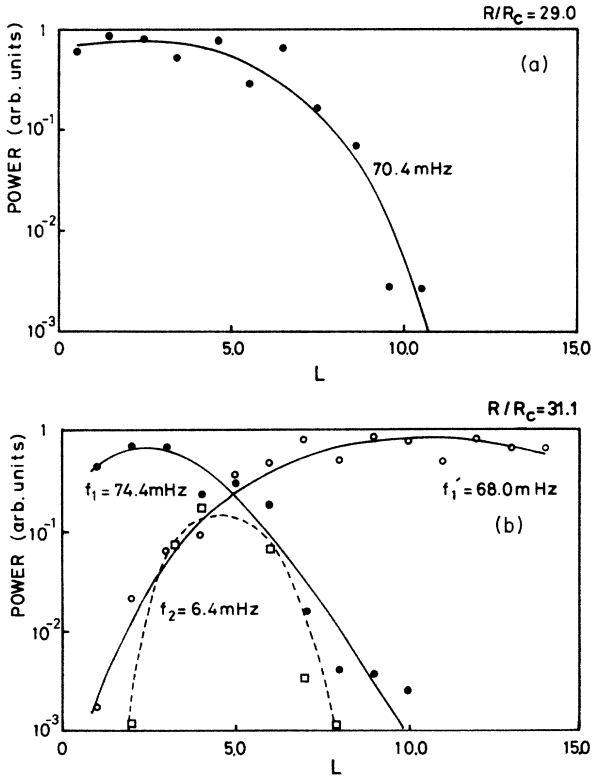

FIG. 1. Spatial distribution of the spectral powers of the characteristic frequencies: (a) periodic oscillation; (b) quasi-periodic oscillation. One of the first type-B modes (frequency $f_2=f_1-f_1'$), indicated by the dotted line, rises in the center of the layer.

Grassberger and Procaccia.[14] The correlation dimension D of an attractor is estimated by the exponent which is given by the asymptotic behavior r^D of the integral correlation function,

$$C(r,N)=\frac{1}{N^2}\sum_{\substack{i,j=1\\ i\neq j}}^{N} H(r-|X_i-X_j|)\,, \tag{1}$$

where $H(r)$ is the Heaviside function and X_i is a vector in d-dimensional phase space obtained from the reconstructed time series by using delay time T. In practice, the correlation integral was evaluated by a random sampling of reference points. The averaged number of points in a ball with radius r for the reference points was calculated to evaluate Eq. (1).

Above the onset of chaos, the estimated correlation dimension becomes nearly constant when d is over 10. But the minimum embedding dimension d_c which is necessary to obtain the dimension of the attractor depends on the delay time. A poor choice of the delay time T breaks the criterion for which an m-dimensional attractor is embedded to a $(2m+1)$-dimensional phase space. If T is much smaller than the value T_i corresponding to the first zero in the autocorrelation function or the value corresponding to the first minimum in the mutual information function,[15] d_c is quite large. When we employed $T=1.22$ sec, which is small in comparison with T_i, d_c was about 40 (T_i is 3.58 sec for the corresponding time series). When T was 3.66 sec, d_c was about 10. We consider that the essential factor determining the properties of embedding of an attractor may be "the embedding time"[16] which is the product of the embedding dimension and the delay time.[17]

It is practical to plot the derivative of the correlation integral with respect to $\log_2 r$ as the function of $\log_2 r$ in order to find the detailed structure of the attractor. Figures 2(a) and 2(b) demonstrate the slopes of the correlation integral versus $\log_2 r$ for two different spatial points with various embedding dimensions. The slope in Fig. 2 was determined by using the least-square method for the subinterval $(\log_2 r-0.4, \log_2 r+0.4)$ of the horizontal axis in the log-log plot of $C(r)$. $C(r)$ was calculated by using 1000 data points and 1000 reference points. In Fig. 2(a) there are two plateaus with a width of a factor of 2. When 30 000 data points and 3000 reference points are used for the computation of $C(r)$, the plateau obtained from the smaller length scale becomes wider to a factor of 3.2 and the width of another plateau barely changes from the width of the plateau obtained by using 1000 data points. We expect that the plateau of the smaller length scale is made wider than a factor of 3.2 by using a much higher number of data points. The width of the plateau of Fig. 2(b) also becomes wider with an increasing number of data points.

Although we may not say that the plateau of the largest length scale implies scaling behavior since it is only a factor of 2 wide, its dependence on the spatial parameter L gives us some information on the structure of fluid motion. It should be noted that two plateaus appeared in Fig. 2(a) and only one plateau appeared in Fig. 2(b), although the same parameters were utilized to evaluate

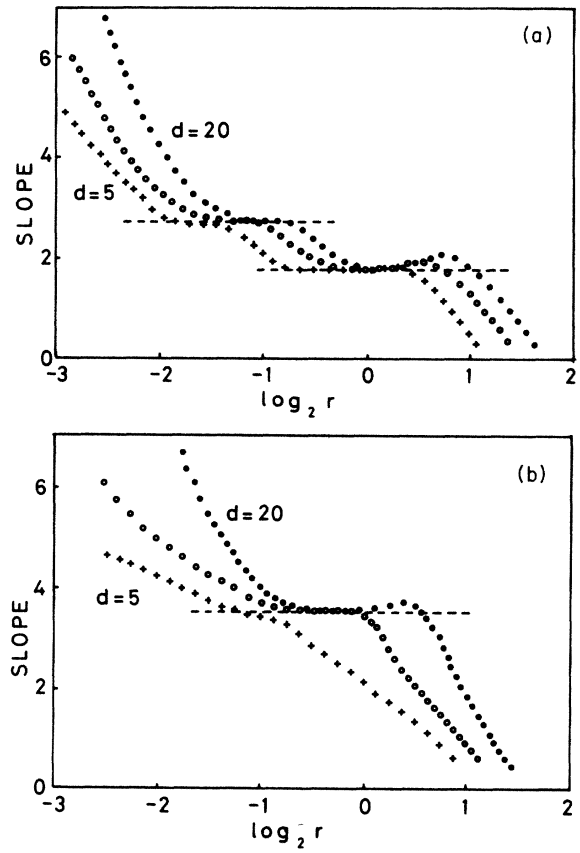

FIG. 2. Curves of the slope of the correlation integral $C(r)$ as a function of $\log_2 r$ for different embedding dimensions $d=5,10,20$ at $R/R_c=34.0$. The values of the plateaus are shown by the dotted lines: (a) for measuring point $L=2.0$, the values of the plateaus are 1.8 and 2.7; (b) for $L=7.0$, only one plateau appeared in the curves. The value of the plateau is 3.6.

$C(r)$. This difference may have originated from the spatially nonuniform oscillation in the fluid layer. Figure 3 summarizes the value of the plateaus in Fig. 2. Near the side walls two plateaus appeared, and in the central part of the layer only one plateau appeared. Inhomogeneity of fluid motion can also be verified from the measurements

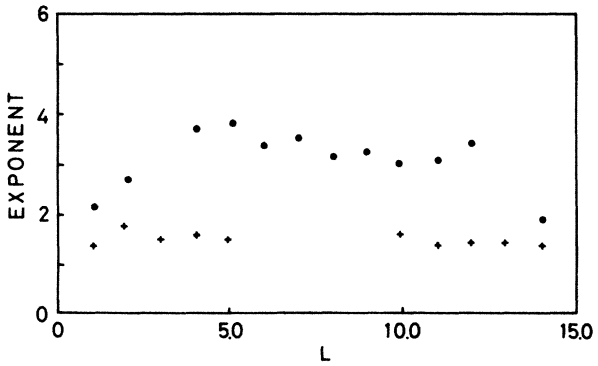

FIG. 3. The values of the plateaus vs L at $R/R_c=34.0$. When multiple plateaus are observed in Fig. 2, the plateau of smaller length scale is indicated by the symbol ● and another plateau is indicated by the symbol +. The plateau of the larger length scale does not correspond to the dimension of the attractor.

of the spatial distribution of the spectral power.

As R is increased continuously from the onset value of chaos, the degree of chaos develops. Figure 4 shows a nonperiodic time series of the temperature gradient at the measuring point $L=7.0$ from $R/R_c=34.7$ to 46.2. In developed chaotic regimes, the correlation dimensions become spatially uniform and no attractor having two characteristic length scales were found. Figures 5(a) and 5(b) show two typical examples of the dimensional values measured in the whole layer for $R/R_c=46.2$ and 50.4, respectively. Each data set contains 30 000 points. The delay time is $T=2.0$ sec and the sampling time is $\tau=0.5$ sec. The deviation of the estimated correlation dimensions from the value of dimensions averaged over the whole layer is smaller than unity in all cases. In order to test the temporal steadiness of the correlation exponent, a long time series containing 10^5 points was measured at the measuring point $L=7.0$ for $R/R_c=52.2$. The time series was divided into five data subsets each containing 20 000 points. We investigated the fluctuation of the correlation exponent for these five data subsets. The averaged dimensional value of five trials is 6.5, and the fluctuation from the averaged value is about 0.6. Therefore, we consider that the deviation of the estimated dimensions in Fig. 5 has mainly originated from the statistical error caused by the finiteness of data sets. However, if the attractors would evolve on much longer time scales than that of our measurements, the estimated dimensions might be much larger and the steadiness of fluid motion may not be verified.

In computation of the correlation dimensions for

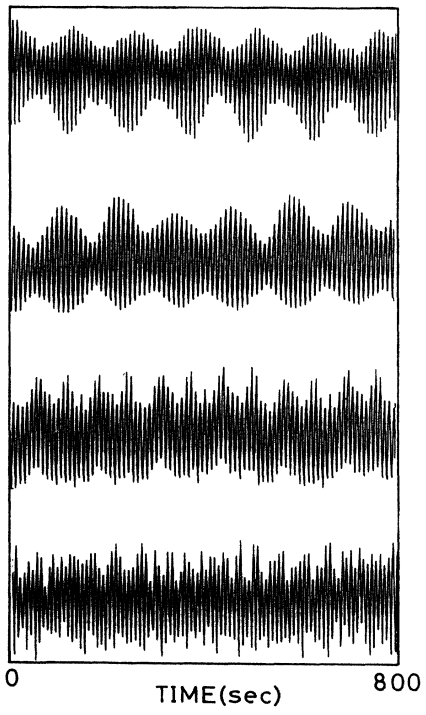

FIG. 4. The change of time series of the temperature gradients at $L=7.0$ with increasing R. The Rayleigh numbers of time series from bottom to top in Fig. 4 are $R/R_c=34.7$, 37.8, 41.8, and 46.2. The amplitude of signals were normalized.

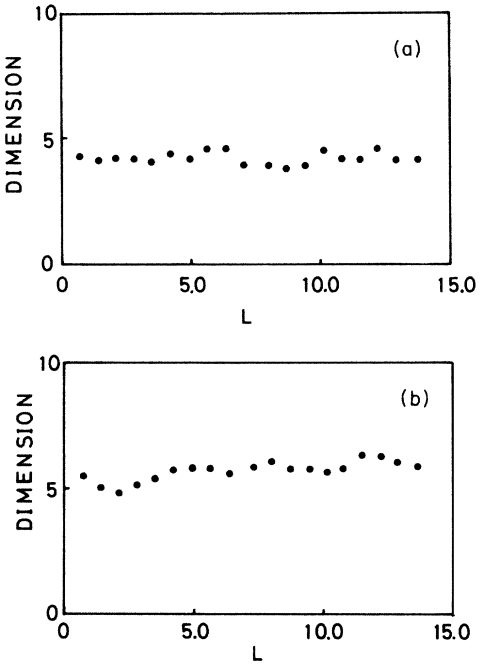

FIG. 5. The correlation exponents vs the distance L for (a) $R/R_c=46.2$ and (b) $R/R_c=50.4$.

developed chaotic attractors where R/R_c is greater than 53, a spurious plateau appeared in the correlation integral as shown in Fig. 6(a). This plateau may lead to inaccurate and spurious estimates of dimension. The appearance of a spurious plateau may be caused by the effect of autocorrelation of chaotic signal in a limited data set. Therefore, we used a modificated version of Eq. (1) proposed by Thieler.[18] The slightly modificated correlation integral is

$$C(r,N,W)=\frac{2}{N^2}\sum_{n=W}^{N}\sum_{i=1}^{N-n}H(r-|X_{i+n}-X_i|)\,, \qquad (2)$$

where $W=1$ gives the standard formula defined by Eq. (1). Equation (2) was evaluated by a random sampling of 150 reference points and by 30 000 data points. For the same data set in Fig. 6(a) the correlation integrals corresponding to various W were computed. The effect of a spurious plateau is negligible at over $W=5$ in our data. Figure 6(b) shows a log-log plot of the correlation integral for $W=10$ as an example. Even if a clear effect of the spurious plateau like Fig. 6(a) is not found in the correlation integral, the estimated dimension obtained from Eq. (1) is slightly corrected by Eq. (2) within a few percent when the dimension of the attractor is about 5. Furthermore, high-dimensional attractors whose dimension is about 9 are obtained from Eq. (2) at $R/R_c=54.6$. But one may not be justified in claiming the validity of the result since the width of the scaling region is only a factor of 2 (Fig. 7).

III. DISCUSSION

We have presented data showing the evolution of the temporal and spatial structure of chaos in an extended

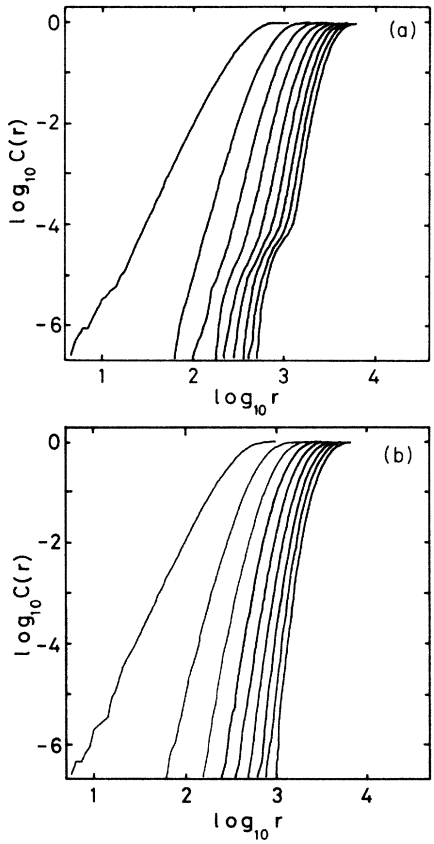

FIG. 6. (a) Log-log plot of the standard Grassberger-Procaccia correlation integral for embedding dimensions $d=4,8,12,\ldots,36$. (b) Log-log plot of the modificated correlation integral defined by Eq. (2) for the same data set of Fig. 6(a) with $W=10$.

Rayleigh-Benard convection system with an aspect ratio of 15.0. The first and subsequent Hopf instabilities occur near the side wall of the container. The distribution of spectral powers is apparently inhomogeneous in the fluid layer in periodic and quasiperiodic regimes. Inhomogeneity of fluid motion also exists just above the onset of chaos, and its structure is reflected in the evaluated correlation integrals. On the other hand, the estimated correlation dimensions in each position of the fluid layer are spatially uniform in developed chaotic regimes.

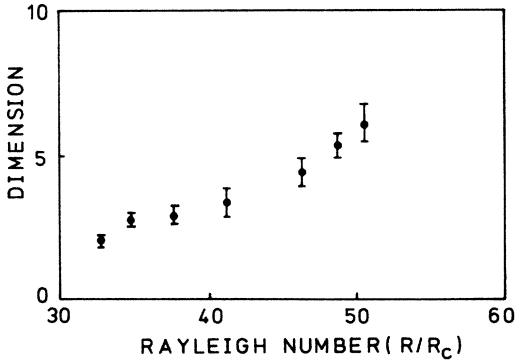

FIG. 7. The development of the correlation dimension as a function of R/R_c at $L=7.0$.

The inhomogeneous distribution of the spectral powers may give rise to attractors whose structure has more than one length scale. In this case an interesting problem occurs in estimating the dimension of the attractor. If one can not measure all the characteristic length scales due to the instrumental noise, the true dimension of the attractor may not be obtained from its correlation integral. The same problem is met in a chaotic system forced by a chaotic modulation with small amplitude. Let us consider the Henon system weakly modulated by the logistic system with amplitude ϵ as an example. We have carried out numerical simulations of this system with additional random noise. The correlation integral at some chaotic state in such a system has two characteristic slopes in the log-log plot. Denote the dimensions of the Henon and logistic attractor by D_1 and D_2, respectively, when both systems are independent of each other. For small ε, one of the slopes for the larger length scale is equal to D_1 and another slope for the smaller length scale is roughly equal to D_1+D_2. The critical length for the crossover is of order ϵ. In the length scale below ϵ the system seems to have a product structure of both systems. However, one can measure the product structure of the forced system only if the additional noise level is sufficiently small in comparison with the amplitude ϵ. When the noise level is also of the order ϵ, the system looks like the Henon system without modulation at the length scale above the noise level. The smallest length scale one can measure determines the "effective dimension," which is calculated for the length scale just above the noise level.

The two-plateau structure (the structure having two slopes in the log-log plot of the correlation integral) is also expected to appear in a diffusively coupled oscillator system when the diffusion constant is small. For the extended Rayleigh-Benard convection system each oscillator of the coupled system may correspond to the spatially localized mode, if it exists, in the fluid layer. From these considerations it is tempting to propose that the two-plateau structure, such as Fig. 2(a), is caused by the spatially localized modes. However, we may not conclude at the present time that the two-plateau structure is caused by spatial localization of modes for the following two reasons. First, the width of the plateau defined by the larger length scale in Fig. 2(a) is not wide enough. Second, the inhomogeneous distribution of the spectral powers does not always mean the existence of independent physical subsystems. Further study is required to identify the spatial localization of modes in chaotic state. Furthermore, experimental studies for more extended convection systems may help us to understand the spatiotemporal structure of spatially distributed systems.

ACKNOWLEDGMENTS

We acknowledge helpful discussions with J. P. Goullub, A. Libchaber, and P. Coullet. We are very grateful to M. Lowe, M. Heutmaker, and K. Miyano for their critical reading of the manuscript. This work is partially supported by the Mitsubishi Science Foundation.

*Present address: The James Frank Institute, University of Chicago, 5640 South Ellis Avenue, Chicago, IL 60637.

[1]J. P. Gollub and S. V. Benson, J. Fluid Mech. **100**, 499 (1980).

[2]J. P. Gollub, S. V. Benson, and J. Steinman, Ann. N.Y. Acad. Sci. **357**, 22 (1980).

[3]M. Giglio, S. Musazzi, and U. Perini, Phys. Rev. Lett. **47**, 243 (1981).

[4]A. Libchaber, and J. Maurer, J. Phys. (Paris) Colloq. **41**, C3-51 (1980).

[5]A. Libchaber, C. Laroche, and S. Fauve, J. Phys. (Paris) Lett. **43**, L-211 (1982).

[6]P. Berge, M. Dubois, P. Manneville, and Y. Pomeau, J. Phys. (Paris) Lett. **41**, L-341 (1980).

[7]M. Dubois, M. A. Rubio, and P. Berge, Phys. Rev. Lett. **51**, 1446, 2345 (1983).

[8]M. Sano and Y. Sawada, in *Chaos and Statistical Methods*, edited by Y. Kuramoto (Springer, Berlin, 1984), p. 226.

[9]B. Malraison, P. Atten, P. Berge, and M. Dubois, J. Phys. Lett. **44**, L-897 (1983).

[10]In the case of Taylor-Couette flow, see A. Brandstater, J. Swift, H. L. Swinney, A. Wolf, J. D. Farmer, E. Jen, and J. P. Crutchfield, Phys. Rev. Lett. **51**, 1442 (1983), and see also A. Brandstater, and H. L. Swinney, Phys. Rev. A **35**, 2207 (1987).

[11]J. P. Gollub, J. F. Steinman, and A. R. MacCarriar, J. Fluid Mech. **125**, 259 (1982).

[12]R. W. Walden, P. Kolodner, A. Passner, and C. M. Surko, Phys. Rev. Lett. **53**, 242 (1984).

[13]G. A. Held and C. Jeffries, Phys. Rev. Lett. **55**, 887 (1985).

[14]P. Grassberger and I. Procaccia, Phys. Rev. Lett. **50**, 346 (1983); Physica **9D**, 189 (1983).

[15]A. M. Fraser and H. L. Swinney, Phys. Rev. A **33**, 1134 (1986).

[16]J. P. Eckmann, S. O. Kamphorst, D. Ruelle, and S. Ciliberto, Phys. Rev. A **34**, 4971 (1986).

[17]The relation of the minimum embedding dimension d_c and the delay time T is studied for the Lorenz system. See S. Sato, M. Sano, and Y. Sawada, Prog. Theor. Phys. **77**, 1 (1987).

[18]J. Theiler, Phys. Rev. A **34**, 2427 (1986).